Modulating TAK1 Expression Inhibits YAP and TAZ Oncogenic Functions in Pancreatic Cancer

Raffaela Santoro[1], Marco Zanotto[1], Francesca Simionato[2], Camilla Zecchetto[2], Valeria Merz[2], Chiara Cavallini[3], Geny Piro[1], Fabio Sabbadini[1], Federico Boschi[4], Aldo Scarpa[5], and Davide Melisi[1,2]

ABSTRACT

YAP and TAZ are central determinants of malignancy; however, their functions remain still undruggable. We identified TGFβ-activated kinase 1 (TAK1) as a central hub integrating the most relevant signals sustaining pancreatic cancer aggressiveness and chemoresistance. Glycogen synthase kinase (GSK)3 is known to stabilize TAK1, and its inhibition causes a reduction in TAK1 levels. Here, we hypothesized that TAK1 could sustain YAP/TAZ program, and thus, modulation of TAK1 expression through the inhibition of GSK3 could impair YAP/TAZ functions in pancreatic cancer.

Differentially expressed transcripts between pancreatic cancer cells expressing scramble or *TAK1*-specific shRNA were annotated for functional interrelatedness by ingenuity pathway analysis. TAK1 expression was modulated by using different GSK3 inhibitors, including LY2090314. *In vivo* activity of LY2090314 alone or in combination with nab-paclitaxel was evaluated in an orthotopic nude mouse model.

Differential gene expression profiling revealed significant association of TAK1 expression with HIPPO and ubiquitination pathways. We measured a significant downregulation of YAP/TAZ and their regulated genes in shTAK1 cells. TAK1 prevented YAP/TAZ proteasomal degradation in a kinase independent manner, through a complex with TRAF6, thereby fostering their K63-ubiquitination versus K48-ubiquitination. Pharmacologic modulation of TAK1 by using GSK3 inhibitors significantly decreased YAP/TAZ levels and suppressed their target genes and oncogenic functions. *In vivo*, LY2090314 plus nab-paclitaxel significantly prolonged mice survival duration.

Our study demonstrates a unique role for TAK1 in controlling YAP/TAZ in pancreatic cancer. LY2090314 is a novel agent that warrants further clinical development in combination with nab-paclitaxel for the treatment of pancreatic cancer.

Introduction

Pancreatic cancer is among the most lethal and inadequately understood human malignancies (1, 2), and will seemingly become the second leading cause of cancer-related death by 2030 in Western countries. Pancreatic cancer patients' prognosis is a dismal, mainly because of the early metastatic behavior of the disease, its aggressiveness, and it is the unique resistance to standard of care chemotherapeutic agents (3).

The transcriptional regulators Yes Associated Protein (YAP) and transcriptional coactivator with a PDZ-binding domain (TAZ) are emerging as central determinants of malignancy, due to their major role in sustaining initiation, progression, metastasis, and chemoresistance of tumors, and inducing cancer stem cells phenotype. In pancreatic cancer, YAP represents a critical oncogenic effector of KRAS-initiated tumor progression (4). The survival of KRAS addicted tumor cells was recently associated to YAP1 activation (5). Moreover, YAP activation was necessary to sustain KRAS-independent spontaneous recurrence of pancreatic cancer developed in $KRAS^{G12D}$ inactivated mice (6). However, the activity of these transcriptional regulators remains still undruggable to date, and just the dissection of the different signaling pathways that sustain their activation could facilitate the development of new therapeutic approaches (7). Although the Hippo pathway is acknowledged as the main regulator of YAP/TAZ, recent studies have identified novel upstream signaling pathways widening the complexity of their regulation (8).

TAK1 is a serine/threonine kinase constituting the cellular hub for several cytokine-mediated signaling, which critically regulates inflammatory responses and cell survival (9, 10) by controlling the activation of transcription factors such as AP-1 and NF-κB (11, 12). We demonstrated that targeting the kinase activity of TAK1 dramatically led to a proapoptotic phenotype and, in turn, to a significantly higher sensitivity to chemotherapy and radiotherapy in pancreatic (13) and esophageal carcinoma (14). Despite the variety of compounds targeting TAK1 kinase activity, none of them has progressed into clinical development to date.

Glycogen synthase kinase (GSK)3 is a multifunctional serine/threonine kinase that is encoded by 2 closely related genes, GSK-3α and GSK-3β. GSK3 has been implicated in a number of human malignancies, including pancreatic cancer. In particular, a recent study demonstrated that GSK-3α interacts with TAK1 thus stabilizing the TAK1–TAB complex. This promotes noncanonical NF-κB signaling in pancreatic cancer cells. Pharmacologic inhibition of GSK-3 caused a significant reduction of TAK1 levels (15).

In this study, we explored novel downstream signaling of TAK1, and hypothesized that this kinase could sustain the essential role of YAP/TAZ program in pancreatic cancer. Thus, targeting TAK1

[1]Digestive Molecular Clinical Oncology Research Unit, Department of Medicine, Università degli studi di Verona, Verona, Italy. [2]Medical Oncology Unit, Azienda Ospedaliera Universitaria Integrata, Verona, Italy. [3]Research Center LURM, Interdepartmental Laboratory of Medical Research, Università degli studi di Verona, Verona, Italy. [4]Department of Computer Science, Università degli studi di Verona, Verona, Italy. [5]ARC-Net Research Centre, University and Hospital Trust of Verona and Department of Diagnostics and Public Health, Section of Anatomical Pathology, University and Hospital Trust of Verona, Verona, Italy.

Note: Supplementary data for this article are available at Molecular Cancer Therapeutics Online (http://mct.aacrjournals.org/).

Corresponding Author: Davide Melisi, University of Verona, AOUI Policlinico, Piazzale L.A. Scuro, 10, Verona 37134, Italy. Phone: 39-04581-28148; Fax: 39-04580-27410; E-mail: davide.melisi@univr.it

Mol Cancer Ther 2020;19:247–57

doi: 10.1158/1535-7163.MCT-19-0270

expression by inhibiting GSK3 could suppress YAP/TAZ expression and modulate, in turn, their contribution to the malignancy and treatment resistance of this disease.

Materials and Methods

Cell cultures and reagents

Human pancreatic cancer cell lines AsPC1, Panc1 were purchased from the ATCC. MDA-Panc28 cell line was a kind gift by Dr. Paul J. Chiao. Panc1, AsPC1, and MDA-Panc28 pancreatic cancer cell lines silenced for the expression of TAK1 were established as described by Melisi and colleagues (13). All cell lines used in this study were cultured as monolayers at 37°C, 5% CO_2 in high glucose DMEM (Catalog No. 41966-029; Life Technologies), supplemented with 10% heat-inactivated FBS (Catalog No. 10270-106; Life Technologies), 2 mmol/L L-glutamine (Catalog No. BE17-605E; Lonza), 100 IU/mL penicillin and 100 μg/mL streptomycin (Catalog No. 15140-122; Life Technologies), and kept in culture for maximum 1 month. All cell lines used in this study were authenticated using DNA fingerprinting at the genomic core facility at Wayne State University (2009) and routinely tested for mycoplasma presence using the MycoAlert Mycoplasma Detection Kit (Catalog No. LT07-118; Lonza).

(5Z)-7-oxozeaenol TAK1 kinase selective inhibitor (TOCRIS Bioscience) was dissolved in 100% DMSO at a stock concentration of 10 mmol/L (16). Lithium chloride (Catalog No. L4408), a nonspecific oral GSK3 inhibitor ($IC_{50} = 10$ mmol/L) was purchased by AppliChem and was dissolved in sterile water at a stock concentration of 5 mmol/L. A working concentration of 20 mmol/L has been used in all the *in vitro* assays. LY2090314 (Catalog No. S7063) and CHIR-99021 (Catalog No. S1263) were purchased from Selleckchem and dissolved in DMSO. Gemcitabine (Accord), oxalipatin (Accord), SN38 (Campto, ref. 17), and nab-paclitaxel (Celgene) were used at the indicated concentrations for the indicated time. The proteasome inhibitor MG132 (Z-Leu-Leu-Leu-al, C2211; Sigma-Aldrich) was dissolved in 100% DMSO and used at a 5 μmol/L concentration for 24 hours. For *in vivo* experiments, LY2090414 was dissolved in 5% Tween-80 (A4743; Applichem) in saline. Drug interactions were studied for synergistic effect according to Chou and Talalay method by CalcuSyn software, as well as to Bliss independence using Chalice Analyzer online (18). Chemical structures for MG-132, LY2090314, and CHIR-99021 are shown in Supplementary Fig. S1A.

Gene expression microarrays and pathway analysis

Total RNA was extracted using TRizol reagent (Catalog No. 15596-018; Life Technologies) following manufacturer's instruction. RNA quality was assessed by agarose gel electrophoresis. Total RNA was quantified by reading the absorbance at 260 nm using a Nanodrop (Thermo Fisher Scientific). Differences in gene expression between control and silenced TAK1 cells were examined using Illumina Human 48k gene chips (D-103-0204; Illumina) as previously described in ref. 19. Briefly, 500 ng total RNA were reverse-transcribed and cRNA was synthesized and biotinylated using the IlluminaTotalPrep RNA Amplification Kit (AMIL1791; Ambion). cRNAs (750 ng) were hybridized using Illumina Human 48k gene chips (Human HT-12 V4 BeadChip). Array were washed with Illumina High Temp Wash Buffer for 10 minutes at 55°C, and stained with streptavidin-Cy3 dyes (Amersham Biosciences). The Illumina Genome Studio software (Genome Studio V2011.1) was used to obtain probe intensity. Raw data were Loess normalized with the Lumi R package and further processed with Excel software. Each microarray experiment was repeated twice. Network and functional interrelatedness were studied for the differentially expressed genes using the Ingenuity Pathway Analyses (IPA) software program (Ingenuity Systems).

Cell transduction

The expression vector for either murine wild-type TAK1 or murine kinase-dead K63W TAK1 (20) and packaging vectors were cotransfected into 293T cells. Seventy-two hours posttransfection, supernatants containing virus were filtered through a 0.45 μm filter (Corning, Inc.). AsPc-1, PANC-1, and MDAPanc-28 cells were transduced by the lentivirus in the presence of the polycation polybrene and lysed 72 hours post infection to obtain cellular extracts.

Reverse transcription and qRT-PCR

Differences in gene expression were measured as described previously (21). Total RNA was extracted using TRizol reagent and quantified by Nanodrop. One microgram o RNA was reverse-transcribed with High Capacity cDNA Reverse Transcription Kit (Catalog No. 4368814; Applied Biosystems) following manufacturer's instruction. cDNA was diluted 1:10 and subjected to RT-PCR using FAST PowerUp SYBR green mastermix (Catalog No. A25742; Applied Biosystems;). Primers were purchased by Life Technologies and used at 0.2 μmol/L final concentration. Changes in gene expression were normalized to β-actin and quantified using the $2^{-\Delta\Delta CT}$ method.

Protein extraction and Western blotting

Western blot analyses were performed as described in ref. 22. Total protein extracts were prepared by lysing cells in radioimmunoprecipitation assay buffer [50 mmol/L Tris HCl (pH 8), 150 mmol/L NaCl, 1% Nonidet P-40, 0.5% sodium deoxycholate, and 0.1% sodium dodecyl sulfate]. All protein extracts were quantified by BCA Protein Assay Kit (23225; Thermo Fisher Scientific) and equal amounts (20–50 μg of protein extract) were loaded onto SDS-PAGE (4%–20%) and transferred to polyvinylidene fluoride membranes (Immobilon-P, Catalog No. IPVH00010; Millipore). Immunoblots were performed using the indicated antibodies. Antibodies to TAK1 (ab109526, 1:1,000), ITCH (ab109018, 1:1,000), TRAF6 (ab94720, 1:1,000), Ub-K63 (ab179434, 1:1,000) were all purchased from Abcam. YAP/TAZ (sc-101199, 1:1,000), CTGF (sc-14939, 1:1,000), GAPDH (sc-166545, 1:50,000) were purchased from Santa Cruz Biotechnology. Secondary anti-mouse and anti-rabbit antibodies were purchased from Santa Cruz Biotechnology. All antibodies were diluted in 3% nonfat dry milk dissolved in Tris-buffered saline (TBS) or 5% BSA/TBS/0.1% Tween-20. Immunoreactive proteins were visualized with Immobilion Western Kit (Catalog No. WBKLS0500; EMD Millipore) according to the manufacturer's instructions. Images were acquired using ImageQuant LAS 4000 mini (GE Healthcare Life Sciences).

Transwell migration assays

Differences in cancer cells migration were measured as described previously (23). Briefly, 5×10^4 cells were allowed to migrate for 20 hours. Following removal of nonmigrating cells, cells migrated to the bottom layer of the transwell insert were stained with DAPI. Each membrane was scanned by fluorescence microscopy (EVOS FL Auto; Thermo Fisher Scientific) and all the cells were automatically counted using ImageJ software. Samples were analyzed in triplicate and percentage of cells relative to control is shown in the graphs. *P* values were calculated by Student *t* test.

Cancer stem cells and colony-forming assays

A total of 5×10^2 cells were seeded in 6 wells plates and grown for 15 days. To maintain good growth conditions, the medium was

changed every 48 hours. Cells were stained for 30 minutes with 0.1% crystal violet dissolved in 10% of formaldehyde. Cells were washed 3 times with water and colonies were counted by automatic microscopy (EVOS FL Auto; Thermo Fisher Scientific). Differences in cancer stem cells were measured as described previously (24).

Nude mouse orthotopic xenograft models

Five-weeks-old female athymic nude mice (Crl:CD1-Foxn1nu, CDNSSFE05S) were purchased from Charles River. Guidelines of the University of Verona Animal Ethic Committee were followed to house animals in specific pathogen-free conditions and treat them. Subconfluent cultures of pancreatic cancer cells were collected using 0.05% trypsin-EDTA (GIBCO; ref. 25300-054). that was inhibited with 10% FBS in DMEM. Tumor cells were resuspended in a solution of 1:1 Matrigel:PBS at 1.0×10^4 cells/μL concentration (Matrigel Matrix Growth Factor; 356230; BD Biosciences). Orthotopic injection of pancreatic cancer cells was performed as previously described in ref. 25. We did not observe anesthesia-related deaths.

Antitumor activity of LY2090314 plus nab-paclitaxel *in vivo* in AsPc1 pancreatic tumor orthotopic xenografts

AsPC1 orthotopic tumor-bearing mice were randomly assigned ($n = 11$ per group) to receive the following on a weekly schedule: (i) vehicle (5% Tween-80 in saline) intraperitoneally (days 1–3–5); (ii) LY2090314 (2.5 mg/kg i.p., days 1–3); (iii) nab-paclitaxel (3 mg/kg i.p., day 5); and their combinations: (4) nab-paclitaxel (3 mg/kg i.p., day 5) plus LY2090314 (2.5 mg/kg i.p., days 1–3). Treatments were continued until progression.

Weight and tumor growth were measured weekly. When a prominent mass was present in the mouse abdomen (tumor volume $\geq$2,000 mm^3), mice were euthanized by cervical dislocation, and that was considered the day of death for survival evaluation. The median survival duration was reached when at least half of the mice in each treatment group were sacrificed.

Immunohistochemistry

Formalin-fixed paraffin-embedded tissue sections were subjected to immunostaining using the streptavidin–peroxidase technique, with diaminobenzidine (Immpact DAB, SK-4105; Vector Lab) as a chromogen, as previously described in ref. 26. Either citrate pH 6.0 (ab93678; Abcam) or Tris-EDTA pH 9.0 (ab93684; Abcam) were used as antigen retrieval buffers. Abcam primary rabbit monoclonal antibodies to Ki67 (ab92742, 1:4,000), YAP (ab205270, 1:2,000), TAZ (ab110239, 1:1,000), CTGF (ab6992, 1:600), AXL (ab72069, 1:100), MMP7 (ab207299, 1:4,000), and CXCR4 (ab124824, 1:500) were used at 4°C overnight to stain sections. Incubation with ImmPRESS HRP Anti-Rabbit IgG Peroxidase Polymer Detection Kit (MP-7401-50; Vector Lab, Burlingame) was performed for 30 minutes; counterstaining was performed with Vector Hematoxylin QS (H-3404; Vector Lab) and slides were mounted using VectaMount Permanent Mounting Medium (H-5000; Vector Lab).

Results

TAK1 prevents YAP/TAZ proteasomal degradation

To identify novel downstream signaling of TAK1 that could drive the aggressiveness of pancreatic cancer, we analyzed differential gene expression (GEO accession number GSE137265, https://www.ncbi.nlm.nih.gov/geo/query/acc.cgi?acc=GSE137265) in AsPC1, Panc1, and MDA-Panc28 pancreatic cancer cell lines transduced with lentivirus expressing *TAK1*-specific shRNA (shTAK1) or scramble sequence as control (**Fig. 1A**) by using the IPA software. We found a significant and consistent association of the genes modulated by TAK1 silencing with the HIPPO, Wnt/β-catenin, and protein ubiquitination pathways (**Fig. 1B**). To deepen our insight into the regulation of the HIPPO pathway, we investigated whether YAP/TAZ expression was affected by TAK1 silencing. We measured a downregulation of YAP/TAZ proteins in stable shTAK1 cells as compared with their respective controls, as well as an upregulation of β-catenin (**Fig. 1C**), which was sustained by increased GSK3α and GSK3β phosphorylation in shTAK1 cell lines as compared with their controls (Supplementary Fig. S1B). Consistently, we measured a significant ($P < 0.01$) downregulation of the YAP/TAZ regulated genes *DKK1*, CTGF, and *AXL* in shTAK1 cells as compared with their respective controls (**Fig. 1D**). The same downregulation of YAP/TAZ was demonstrated in cells transiently transfected with siRNA sequences targeting *TAK1* (Supplementary Fig. S1C), which corroborated our findings and ruled out the possibility that this could be due to shTAK1 off-target and/or long-term adaptive effects. However, when we measured *YAP/TAZ* mRNA levels, we did not observe a consistent significant downregulation of these genes in stable shTAK1 cells. A significant upregulation of *YAP/TAZ* mRNA levels was measured in MDA-Panc28 cells silenced for TAK1 expression as compared to their respective controls, which we interpreted as a compensatory effect (**Fig. 1E**).

To test whether the modulation of YAP/TAZ by silencing of TAK1 could be related to TAK1 kinase activity, we treated AsPC1, Panc1, and MDA-Panc28 pancreatic cancer cell lines with the TAK1 kinase inhibitors (5Z)-7-oxozeaenol. Effective inhibition of TAK1 kinase activity was confirmed by suppression of IKK phosphorylation and decrease in BIRC3 levels (Supplementary Fig. S2A). However, the inhibition of TAK1 kinase activity did not decrease YAP/TAZ protein levels in the 3 pancreatic cancer cell lines under investigation (**Fig. 2A**). Conversely, when we transduced stable shTAK1 cells with a murine K63W TAK1 kinase dead expressing vector, which could not be targeted by human-specific shRNA sequences, we measured a significant rescue of the downregulation of YAP/TAZ proteins at levels similar to those obtained by transducing them with a wild-type murine TAK1 sequence. Moreover, this rescue contributed to rule out potential shTAK1 off-target effects (**Fig. 2B**). Altogether, these results demonstrate that the expression of TAK1, rather than its kinase activity, could affect YAP/TAZ stability.

In this regard, we investigated whether proteasomal degradation could be involved in TAK1-mediated modulation of YAP/TAZ protein stability. Treatment with proteasome inhibitor bortezomib increased YAP/TAZ protein levels in all these cell lines. Interestingly, although we observed only a modest increase in YAP/TAZ protein levels in control cell lines, YAP/TAZ were strongly upregulated in shTAK1 cells upon proteasomal inhibition with both bortezomib (**Fig. 2C**) and MG-132 (Supplementary Fig. S2B). We investigated, thus, whether silencing of TAK1 could modulate the expression of either K48 or K63 ubiquitin ligases. We measured lower protein levels of TRAF6 and higher protein levels of ITCH in shTAK1 cells than in their respective controls (**Fig. 2D**), as well as a decrease in total K63 ubiquitinated proteins in shTAK1 cells than in their respective controls (Supplementary Fig. S3A). Hence, we performed specific K63-linked and K48-linked precipitations and we observed a decrease of K63-linked and an increase in K48-linked ubiquitinated YAP/TAZ in shTAK1 cells as compared with their respective control (**Fig. 2E**). Accordingly, YAP/TAZ immunoprecipitation followed by specific anti-K48 and anti-K63 ubiquitin immunoblot showed an increase in K48-ubiquitinated and a decrease in K63-ubiquitinated YAP/TAZ in cells silenced for TAK1 (**Fig. 2F**). To corroborate our data, we performed

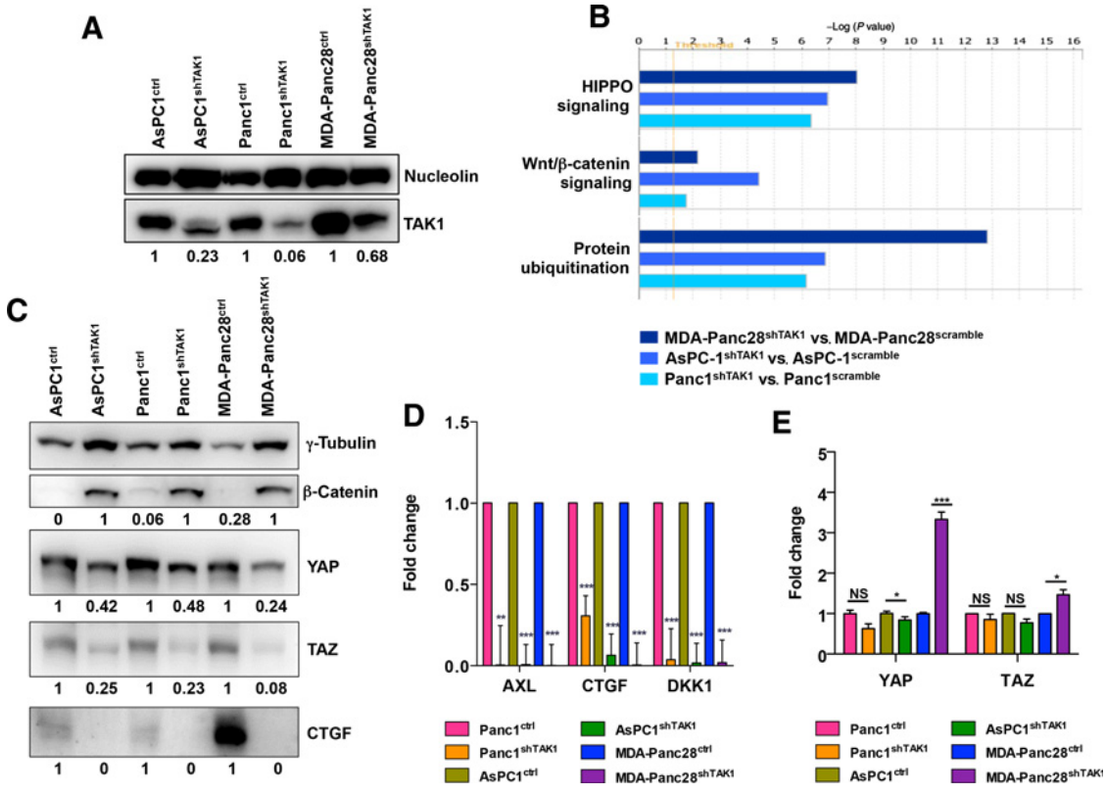

Figure 1.

Identification of TAK1-regulated pathways. **A,** Immunoblot analysis of the indicated cellular extracts. Numbers indicate the normalized ratio of TAK1 over nucleonin signals obtained by densitometric analysis. **B,** Representation of selected TAK1-regulated pathways. Histograms show the significance values for the canonical pathways as calculated by Fisher exact test right-tailed. Blue bars indicate predicted pathway inhibition (*z*-score) in shTAK1 cells as compared with their respective controls. **C,** Immunoblot analysis of the indicated cellular extracts. Numbers indicate the normalized ratio of the indicated proteins over γ-tubulin signals obtained by densitometric analysis. **D** and **E,** Microarray data validation by qRT-PCR. Histograms show fold change in RNA expression between the gene of interest and *β-actin*. Error bars indicate SD. NS, nonsignificant; *, $P < 0.05$; **, $P < 0.01$; ***, $P < 0.001$.

co-immunoprecipitations in AsPC1, Panc1, and MDA-Panc28 cells and we demonstrated the existence of a protein complex between YAP/TAZ and TRAF6 (Supplementary Fig. S3B). Notably, we demonstrated that the presence of TAK1 was necessary for the formation of the YAP/TAZ–TRAF6 complex (**Fig. 2G**).

Altogether, these data demonstrate that, independently by its kinase activity, TAK1 protein levels can regulate YAP/TAZ protein stability by fostering their K63-ubiquitination versus K48-ubiquitination through the binding with TRAF6, thus preventing their proteasomal degradation.

Modulating TAK1 levels through GSK3 inhibition reduces YAP/TAZ protein levels and activities

To translate our findings into a therapeutic approach relevant for patients presenting with pancreatic cancer, we took advantage of the observation by Bang and colleagues (15) that GSK3 inhibition could reduce TAK1 stability. Thus, we hypothesized that GSK3 inhibition could be used to achieve a TAK1-mediated downregulation of YAP/TAZ proteins.

To obtain a pharmacologic modulation of TAK1 expression, we used 2 potent and highly selective inhibitors of GSK3α/β, LY2090314 and CHIR-99021, and the unselective GSK3 inhibitor LiCl, which acts in an uncompetitive manner by displacing a divalent cation required for GSK3 catalytic activity (27). This resulted in a substantial decrease of YAP/TAZ and TAK1 protein levels in all the 3 pancreatic cancer cell lines (**Fig. 3A**; Supplementary Fig. S4A). Treatment with the proteasome inhibitor Bortezomib partially restored TAK1 and YAP/TAZ protein levels (**Fig. 3A**). Similar to the *TAK1* silencing, modulation of TAK1 expression induced by GSK3 inhibition resulted in a significant downregulation of YAP/TAZ regulated genes *CTGF*, *AXL*, and *CYR61* in all the 3 pancreatic cancer cell lines ($P < 0.05$; **Fig. 3B**; Supplementary Fig. S4B). As obtained by silencing TAK1 expression, treatment with LY2090314 increased levels of GSK3 target β catenin (Supplementary Fig. S4C). Similar effects were confirmed in FLO-1 and KYAE-1 esophageal cancer cell lines (Supplementary Fig. S5A and S5B).

YAP/TAZ are known as important mediators of cell proliferation, migration, anchorage-independent growth, and stemness (8); thus, we evaluated whether modulation of TAK1 expression induced by GSK3 inhibition would impair these processes. Indeed, we demonstrated that the selective GSK3 inhibitor LY2090314 significantly reduced cell proliferation in control pancreatic cancer cell lines in the same extent than did *TAK1* silencing, while it was ineffective on *TAK1* silenced counterpart (**Fig. 3C**). Moreover, the inhibition of GSK3 significantly reduced clonogenic potential (AsPC1, $P < 0.001$; Panc1, $P < 0.001$; MDA-Panc28, $P < 0.01$; **Fig. 3D**), and consistently and significantly impaired the migration ability of AsPC1, Panc1, and MDA-Panc28 cells ($P < 0.05$; **Fig. 3E**). Conversely, LY2090314 was completely

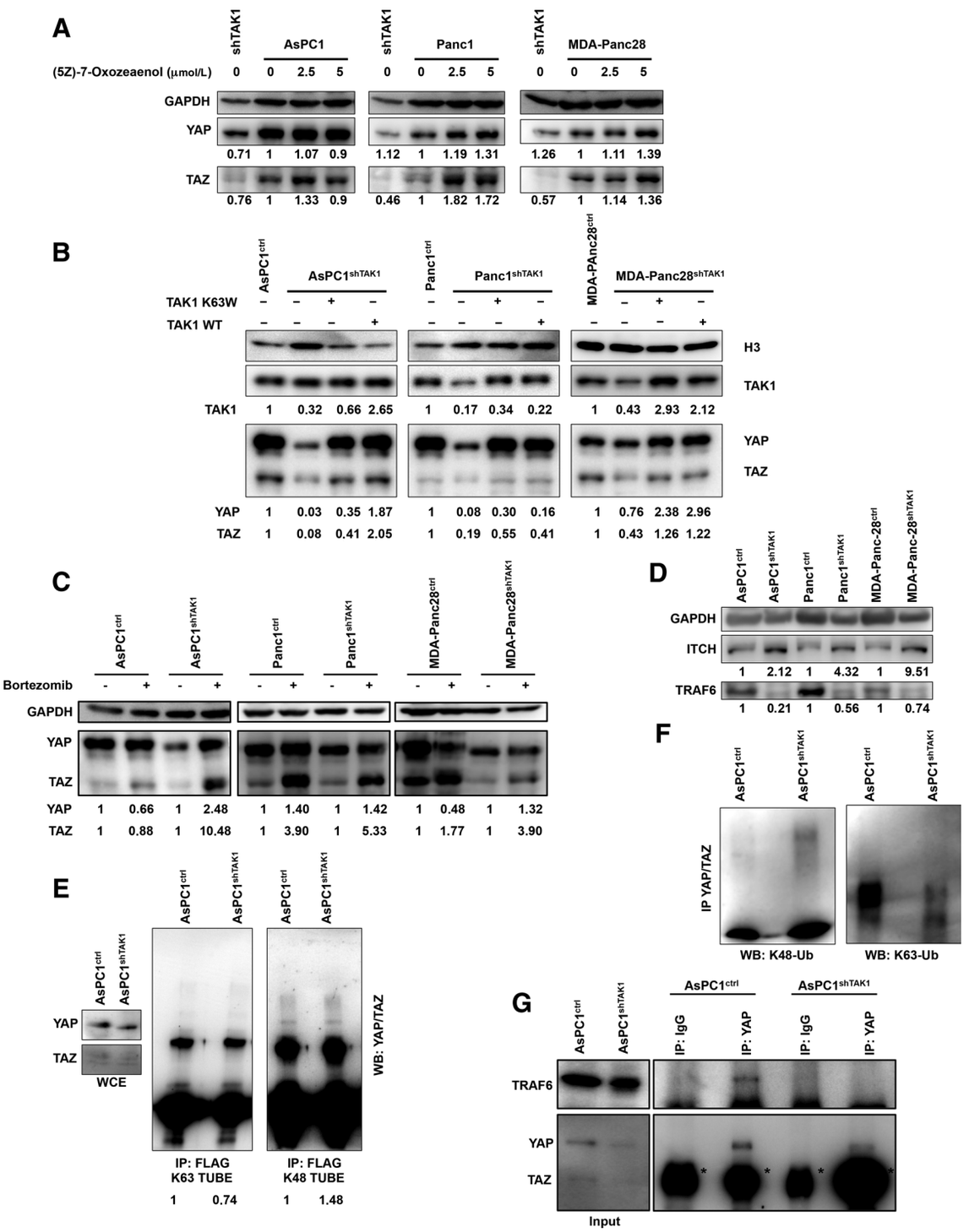

Figure 2.

TAK1 modulates YAP and TAZ ubiquitination. **A,** Immunoblot analysis of cells treated for 48 hours with the TAK1 kinase inhibitor (5Z)-7-oxozeaenol. Numbers indicate the normalized ratio of YAP/TAZ over GAPDH signals obtained by densitometric analysis. **B,** Immunoblot analysis of cells transduced with either K63W kinase-dead or wild-type TAK1. Numbers indicate the normalized ratio of YAP/TAZ over H3 signals obtained by densitometric analysis. **C,** Immunoblot analysis of cells treated with the proteasome inhibitor bortezomib. Numbers indicate the normalized ratio of YAP/TAZ over GAPDH signals obtained by densitometric analysis. **D,** ITCH and TRAF6 protein levels in the indicated cellular extracts. Numbers indicate the normalized ratio of the indicated proteins over GAPDH signals obtained by densitometric analysis. **E,** Assessment of YAP/TAZ ubiquitination by K63 and K48 specific pull-down in the indicated cell lines. **F,** Immunoblot analysis of immunoprecipitated YAP/TAZ using anti-K48– and anti-K63–specific antibodies in the indicated cell lines. Numbers indicate densitometric analysis. **G,** Immunoblot analysis of YAP/TAZ immunoprecipitated complexes using the indicated antibodies. Asterisks indicate IgG heavy chains.

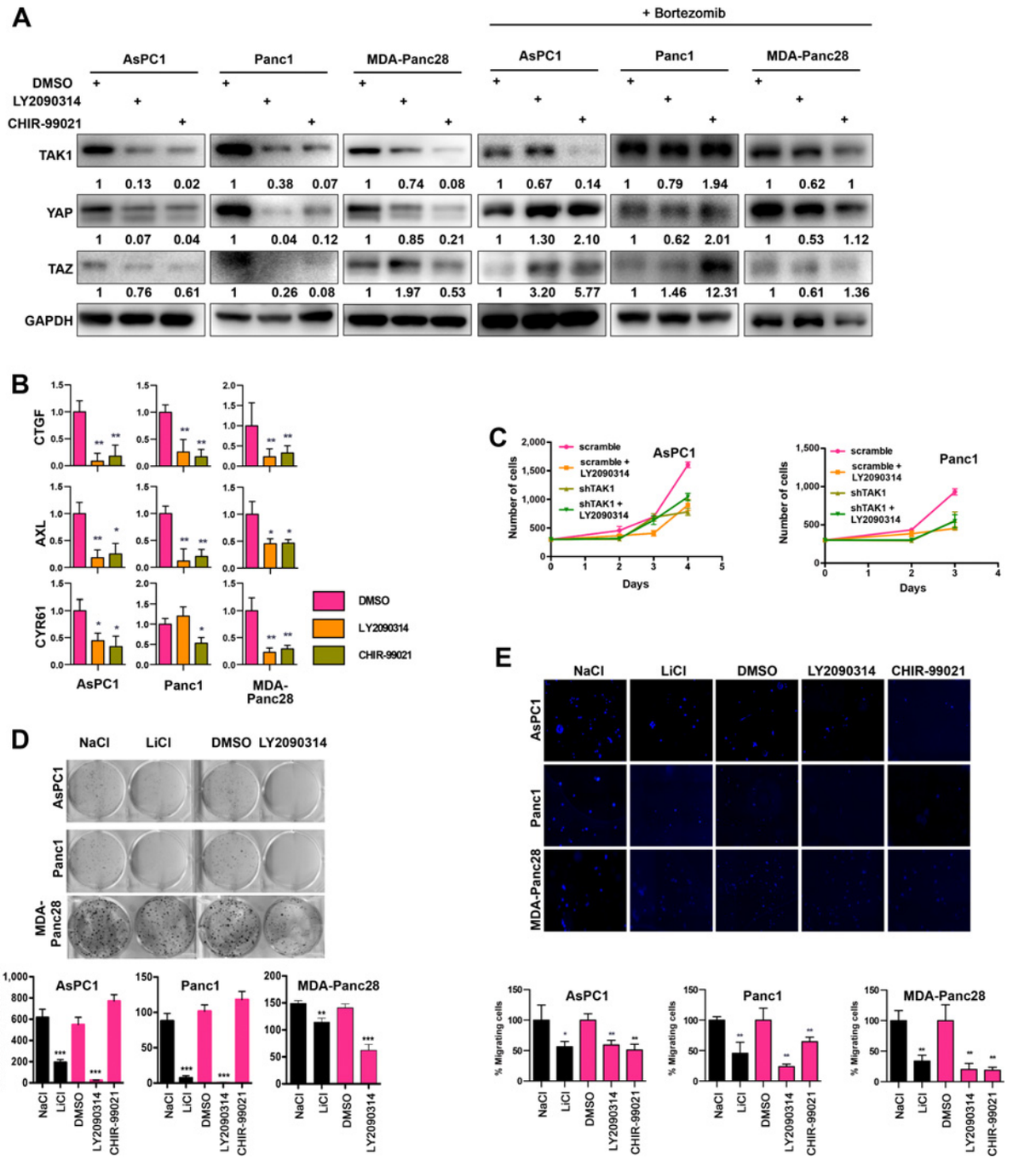

Figure 3.

Pharmacologic inhibition of TAK1 by targeting GSK3 impairs YAP and TAZ levels and oncogenic activities. **A,** Immunoblot analyses of AsPC1, Panc1 e MDA-Panc28 cell lines treated with the GSK3 inhibitors LY2090314 or CHIR-99021 for 72 hours. Cell extracts were subjected to immunoblot with the indicated antibodies. Numbers indicate the normalized ratio of the indicated proteins over GAPDH signals obtained by densitometric analysis. **B,** mRNA expression levels of the indicated YAP/TAZ target genes over *β-actin* from cells treated as in **A**. Error bars indicate SD. *, $P < 0.05$; **, $P < 0.01$. **C,** Growth curves of ctrl and shTAK1 AsPC1 and Panc1 cell lines treated with LY2090314 3 μmol/L. Means and SD of measurements performed in quadruplicate are shown. **D,** Colony formation assays of AsPC1, Panc1, and MDA-Panc28 treated with LiCl 20 mmol/L, LY2090314 3 μmol/L, or CHIR-99021 3 μmol/L for 72 hours, and allowed to form colonies. A representative image of colonies is shown on the left. Histograms show colony number. Error bars indicate SD. **, $P < 0.01$; ***, $P < 0.001$. **E,** AsPC1, Panc1, and MDA-Panc28 cells were seeded and either treated or not with LiCl 20 mmol/L, LY2090314 3 μmol/L, or CHIR-99021 3 μmol/L for 72 hours. Cells were then counted and seeded into the upper chamber of a transwell. Sample images of migrated cells are shown. Histograms show the percentage of migrated cells. Error bars indicate SD. *, $P < 0.05$; **, $P < 0.01$.

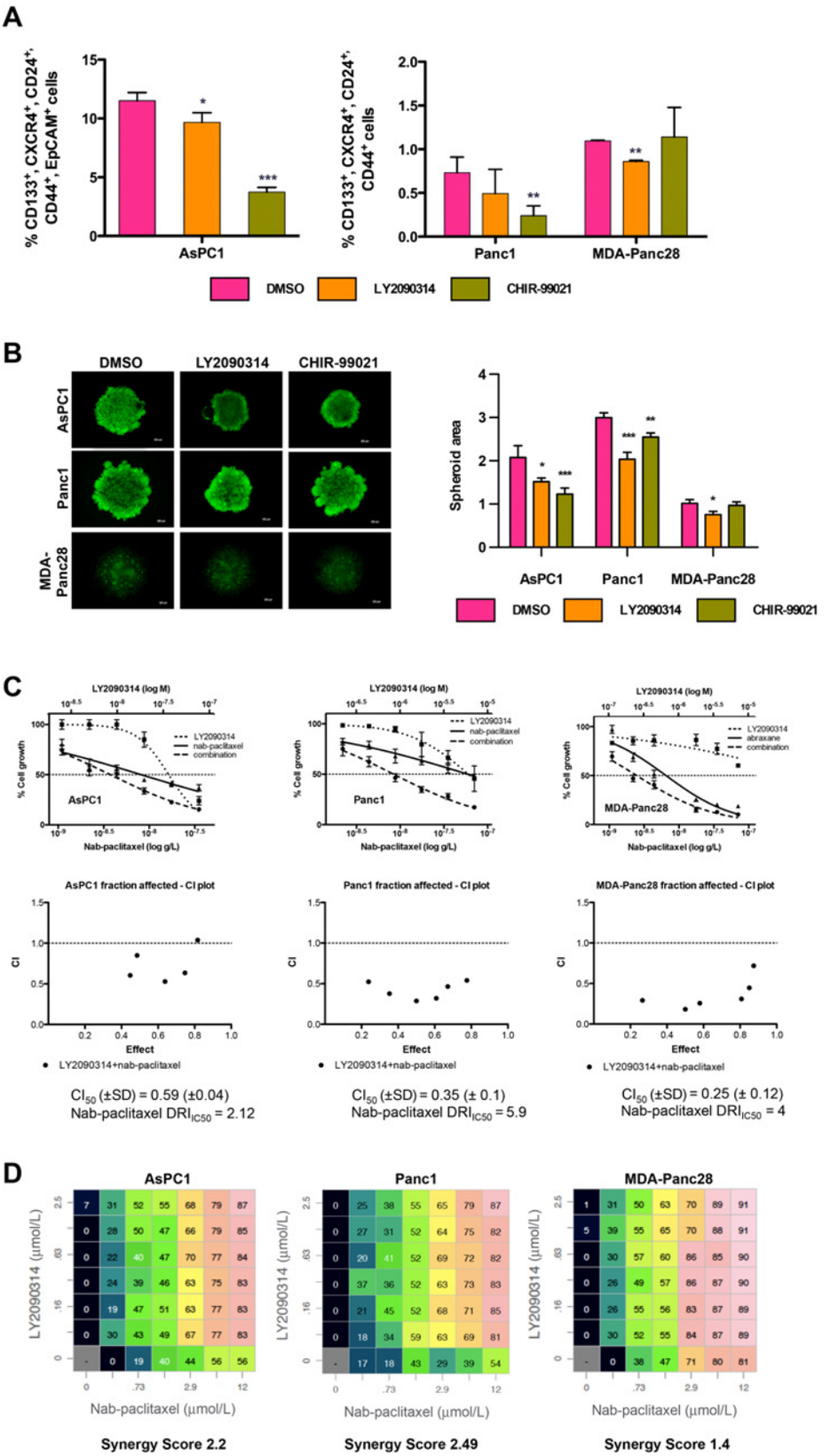

Figure 4.

Targeting GSK3 reduces cancer stem cells features and chemoresistance of pancreatic cancer cell lines. **A,** AsPC1 (left histogram), Panc1, and MDA-Panc28 (right histograms) cell lines were pulsed for 72 hours with the indicated GSK3 inhibitors. 5×10^3 cells were then seeded into ultra-low attachment 6-well plates and cultured in spheroids-forming medium for 52 days. Histograms show the percentage of $CD133^+$, $CXCR4^+$, $CD24^+$, and $CD44^+$ CSCs for Panc1 and MDA-Panc28–derived spheroids and $CD133^+$, $CXCR4^+$, $CD24^+$, $CD44^+$, and $EpCAM^+$ CSCs for AsPC1, as measured by flow cytometry. Error bars indicate SD. *, $P < 0.05$; **, $P < 0.01$; ***, $P < 0.001$. **B,** AsPC1, Panc1, and MDA-Panc28 cells were either treated or not with LY2090314 3 μmol/L or CHIR-99021 3 μmol/L for 72 hours. 20×10^3 cells were then seeded into ultra-low attachment 96 wells plates in triplicate for 15 days to allow for spheroid formation. Pictures show Z-stack microphotographs of representative wells. Histograms show the average area of spheroids formed in each well. Error bars indicate SD. *, $P < 0.05$; **, $P < 0.01$; ***, $P < 0.001$. **C,** AsPC1, PANC1, and MDA-Panc28 cells were pretreated with LY2090314 3 μmol/L or dimethyl sulfoxide (DMSO) as control for 72 hours, and subsequently treated with equitoxic increasing doses of nab-paclitaxel and washed-out after 24 hours. Sulforhodamine B (SRB) assay was used to obtain relative estimates of viable cell number. Means and 95% confidence intervals are shown. Curves were fitted by nonlinear regression analysis. Combination index (CI) plot representing a quantitative measure of the degree of drug interaction for a given end point of the effect measurement is shown. **D,** Data were analyzed for Bliss independence. Dose matrix and synergy score are shown for each cell line.

Table 1. Combination study for nab-paclitaxel and LY2090314.

	CI_{25} (±SD)	CI_{50} (±SD)	CI_{75} (±SD)	DRI_{IC25} nab-paclitaxel	DRI_{IC50} nab-paclitaxel	DRI_{IC75} nab-paclitaxel	DRI_{IC25} LY2090314	DRI_{IC50} LY2090314	DRI_{IC75} LY2090314	*r*
AsPC1	1.6 ± 0.5	0.59 ± 0.1	0.77 ± 0.3	0.6	2.12	7.1	40.2	7.9	1.6	0.99
PANC1	0.44 ± 0.06	0.35 ± 0.04	0.47 ± 0.08	2.8	5.9	12.7	12.5	5.6	2.5	0.99
MDA-Panc28	0.19 ± 0.1	0.25 ± 0.12	0.37 ± 0.24	5.9	4	2.6	60.5	1,223	24,800	0.98

Abbreviations: CI, combination index; DRI, dose reduction index; ED, effect dose; *r*, linear correlation coefficient.

ineffective in shTAK1 pancreatic cancer cell lines (Supplementary Fig. S6A and S6B).

GSK3 inhibition impaired stemness as measured by a significant reduction in both the percentage of $CD133^+$, $CXCR4^+$, $CD24^+$, and $CD44^+$ cancer stem cells ($P < 0.05$; **Fig. 4A**), and a decrease in the area of spheroids growing in low-anchorage conditions ($P < 0.05$; **Fig. 4B**) in all 3 pancreatic cancer cell lines, with the exception of CHIR-99021-treated MDA-Panc28.

Altogether, these data demonstrate that GSK3 inhibition impairs *in vitro* the aggressiveness of pancreatic cancer cells by targeting the more relevant oncogenic functions sustained by YAP and TAZ.

GSK3 inhibitor LY2090314 modulates pancreatic cancer chemoresistance by targeting the TAK1–YAP/TAZ axis

To test our hypothesis that the pharmacologic inhibition of GSK3 could be used to modulate the chemoresistance of pancreatic cancer by impairing YAP/TAZ prosurvival activities, including suppression of apoptosis as previously published in ref. 28, we initially demonstrated that the addition of LY2090314 resulted in an increase of Annexin V+ cells (Supplementary Fig. S7A) and PARP-1 cleavage (Supplementary Fig. S7B). AsPC1, Panc1, and MDA-Panc28 pancreatic cancer cells were, then, treated with increasing doses of classic chemotherapeutic agents nab-paclitaxel, gemcitabine, oxaliplatin, or the active metabolite of irinotecan SN-38 in combination with LY2090314, or DMSO as control. We demonstrated a highly synergistic effect between LY2090314 and these chemotherapeutic agents against the 3 different pancreatic cancer cell lines (**Fig. 4C** and **D**; **Table 1**; Supplementary Fig. S8A–S8C). Combination treatment of LY2090314 plus nab-paclitaxel resulted in a significant increase in PARP-1 cleavage (Fig. S7C). Contrariwise to the effect observed in pancreatic cancer cells, we measured a significant protective effect of LY2090314 on the cytotoxic activity of nab-paclitaxel in HPDE normal human pancreatic duct epithelial cells (Supplementary Fig. S7D).

To demonstrate that LY2090314 could cooperate with clinically relevant doses of nab-paclitaxel into an effective therapeutic approach to inhibit the growth of pancreatic cancer *in vivo*, we used an orthotopic xenograft nude mouse model. Forty mice were orthotopically injected with AsPC1 human pancreatic cancer cells and randomly assigned to 4 treatment groups ($n = 10$ per group). At the median survival duration of mice in the control group (day 62), LY2090314 and nab-paclitaxel as single agents were completely inactive. However, a statistically significant reduction in tumor volume was measured in the mice treated with their combination if compared with untreated controls ($P < 0.05$; **Fig. 5A**). Accordingly, we measure a statistically significantly prolonged median survival duration only in mice treated with the LY2090314 plus nab-paclitaxel combination [**Fig. 5B**, median survival (days): control = 62; nab-paclitaxel = 64; LY2090314 = 62; LY2090314 plus nab-paclitaxel = 105, $P < 0.05$]. All regimens were well tolerated. We did not observe weight loss or other signs of toxicity (Supplementary Fig. S8D).

To confirm that the effects of LY2090314 treatment *in vivo* could be related to the modulation of the TAK1–YAP/TAZ axis, we assessed the expression of YAP/TAZ target genes in tumor specimens excised from mice belonging to the control and LY2090314 groups. As expected, we measured a relevant increase of the inhibitory Ser-21 phosphorylation of GSK3α in mice treated with LY2090314 (**Fig. 5C**). Ser-9 phosphorylation of GSK3β was also induced, although to a lesser extent. Consistently with the results *in vitro*, GSK3 inhibition led to a measurable decrease in TAK1 and YAP/TAZ protein expression and, in turn, to a reduction of the number of $Ki67^+$ cells, and to a substantial decrease of the expression of the YAP/TAZ regulated proteins AXL, CTGF, MMP7, and α-SMA (**Fig. 5C**).

Altogether, these data demonstrated that the downregulation of the expression of TAK1 obtained by using LY2090314 is a valid approach to reduce YAP/TAZ protein levels *in vitro* and *in vivo* and, in turn, to modulate the intrinsic chemoresistance of pancreatic cancer.

Discussion

In this study, we aimed to identify novel intracellular signaling pathways regulated by TAK1. To our knowledge, this is the first study to demonstrate that TAK1 regulates YAP and TAZ activity by inhibiting their K48-linked ubiquitination and proteasomal degradation in a kinase independent manner. In addition, we demonstrated that the downregulation of the expression of TAK1 through the inhibition of GSK3 is able to largely reduce YAP/TAZ protein levels and, in turn, the transcription of the most relevant YAP/TAZ regulated genes both *in vitro* and *in vivo*. In particular, the GSK3 inhibitor LY2090314 proved significantly and consistently effective in decreasing viability, clonogenicity and CSC phenotype in 3 different models of pancreatic cancer cell lines. Most importantly, treatment with LY2090314 sensitized pancreatic cancer cells to the clinically relevant chemotherapeutic agents nab-paclitaxel, gemcitabine, oxaliplatin, and SN38 *in vitro*, and it potentiated the effects of nab-paclitaxel in inhibiting the growth of an *in vivo* orthotopic model of pancreatic cancer.

In recent years, several evidences suggested a putative integration of TAK1 and YAP/TAZ, especially in orchestrating canonical and noncanonical WNT signaling. YAP and TAZ have been demonstrated as integral components of the β-catenin destruction complex, which serves as their functional sink. Activation of canonical WNT signaling causes rapid release of YAP/TAZ, leading to the activation of their transcriptional program. Moreover, the presence of YAP/TAZ in the destruction complex is necessary for the recruitment of βTrCP and β-catenin degradation (29). Conversely, in a noncanonical WNT pathway, Wnt5a induces a G-protein–mediated inhibition of LATS kinase activity towards YAP/TAZ. In turn, the stable YAP/TAZ/TEAD

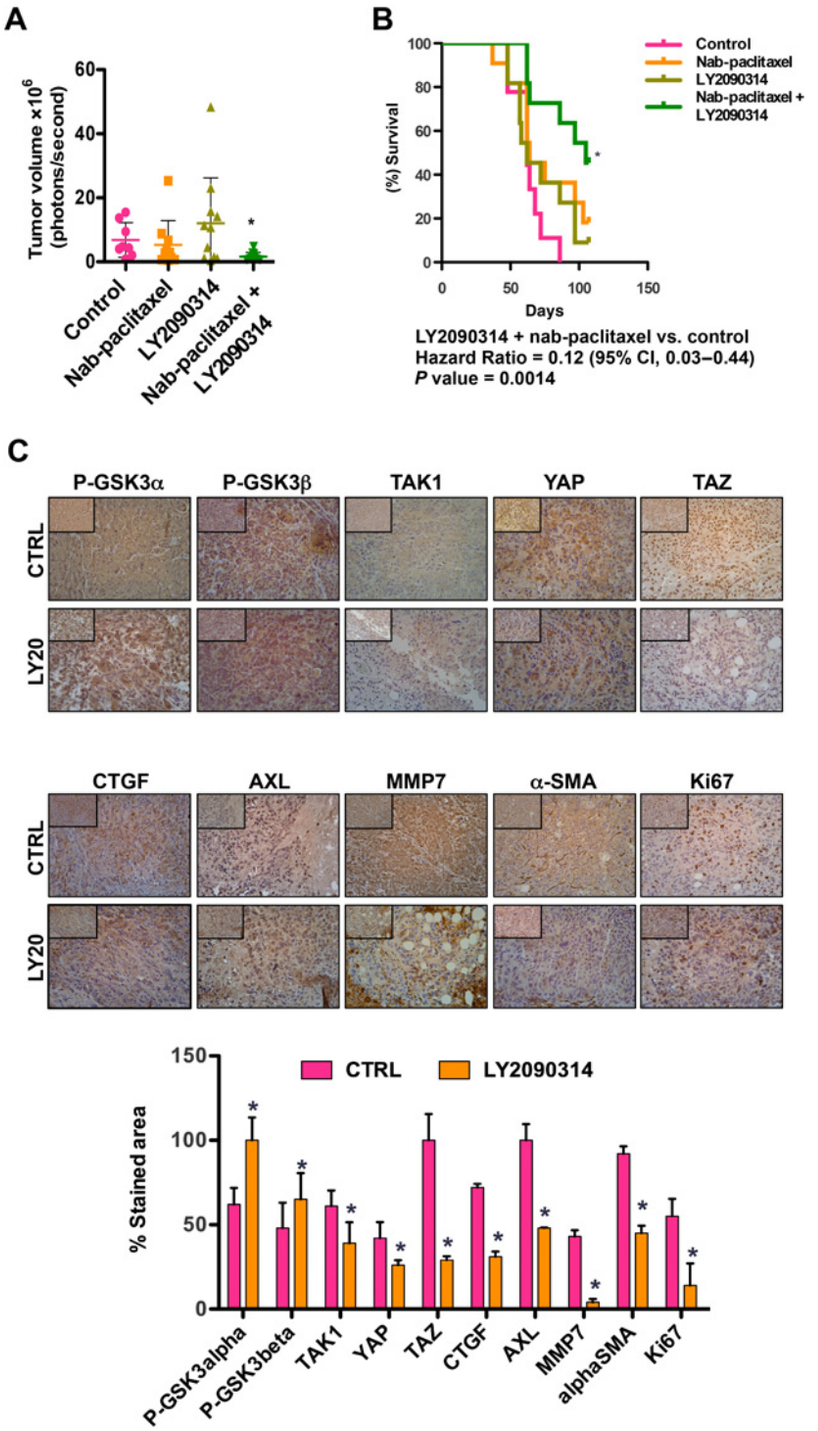

Figure 5.

Antitumor activity of LY2090314 plus nab-paclitaxel *in vivo* in AsPC1 pancreatic tumor orthotopic xenografts ($n = 10$ mice per group). **A,** Tumor volume was quantified as the sum of all detected photons within the region of the tumor per second. Error bars indicate SD. *, $P < 0.05$, as determined by *t* test. **B,** Mice were euthanized by cervical dislocation when presented evidence of advanced bulky disease. Survival was estimated since the day of orthotopic pancreatic cancer cells injection until the day of death. Differences among survival duration of mice in each group were determined by log-rank test. *, $P < 0.05$. **C,** Immunohistochemical analyses. FFPE sections from AsPC1 tumors treated as indicated were stained with the indicated antibodies. 25× magnification images are shown; image inserts show 10× magnification of the same section. Histograms show percentage DAB stained area for 3 independent IHC slides. *, $P < 0.05$.

transcription complex drives the transcription of secreted factors such as DKK1, which inhibit canonical WNT pathway (30). In this regard, TAK1 has been shown to mediate also noncanonical WNT signaling. TAB1-dependent autophosphorylation and activation of TAK1 were induced by Wnt1 stimulation, thus activating a Nemo-like kinase (NLK)–MAPK cascade, and resulting in a TCF/LEF-dependent destabilization of the β-catenin/TCF complex interaction with DNA (31, 32). The noncanonical Wnt5a/$Ca2^+$ pathway activates TAK1–NLK–MAPK cascade as well, resulting in inhibition of canonical β-catenin signaling. However, the Wnt5a-mediated β-catenin inhibition was only minimally affected by overexpression of a kinase-inactive mutant of TAK1(K63W) (33). In a different study, expression of Wnt5A did not induce TAK1 kinase activity or TCF phosphorylation (31). More recently, noncanonical Wnt2 pathway was shown to activate TAK1, which triggered metastasis-associated survival signals in circulating tumor cells from pancreatic cancer patients (34). In this article, we

demonstrated that silencing *TAK1* induces an inhibitory phosphorylation of both GSK3α and GSK3β, which in turn stabilize β-catenin. However, the mechanistic role of TAK1 in the activation of *TAZ/YAP* remained still unexplored to date. In this study, we demonstrated that TAK1 protein levels can regulate YAP/TAZ protein stability by fostering their K63- vs. K48-ubiquitination thus preventing their proteasomal degradation. This mechanism mediated by TAK1 is independent by its kinase activity, and depends on the differential modulation of the K63 E3 ubiquitin ligase TRAF6 and of the K48 E3 ubiquitin ligase ITCH.

Although the frequent aberrant activity of YAP/TAZ in a variety of human cancers candidates these factors as ideal therapeutic targets, the HIPPO cascade remains largely undruggable. Several other approaches have been attempted to inhibit different signaling pathways controlling YAP/TAZ, including Rho/Rock and WNT, but selectivity and toxicity of these agents represented serious limits for their clinical development (35). More recently, the SREBP/mevalonate pathway was also demonstrated to control YAP/TAZ activity, and the inhibition of the rate-limiting enzyme of this pathway (HMG-CoA reductase) by statins inhibited YAP/TAZ localization to the nucleus and the activation of their transcriptional program (36). Although some epidemiologic studies suggest a benefit from the addition of statins to standard treatment regimens in patients with breast cancer and prostate cancer, prospective clinical trials are still required to further define the actual efficacy of this approach (37). In this prospective, LY2090314 is a potent and selective ATP-competitive inhibitor of GSK3 already in clinical evaluation for cancer therapy. The safety of LY2090314 as single-agent treatment or in combination with pemetrexed and carboplatin was initially evaluated in a first-in-human phase I dose-escalation study, in patients with advanced solid tumors (38), and in an open-label phase II study in patients with acute myeloid leukemia (39). Interestingly, an upregulation of β-catenin was measured in peripheral blood mononuclear cells, indicating that LY2090314 had an on-target effect on GSK3 inhibition.

This study, however, has some limitations. The pharmacologic inhibition of GSK3 that we used to achieve a reduction in TAK1 stability could have potentially a direct effect on YAP/TAZ level, regardless of the contribution of TAK1 in this pathway. In particular, it has been recently demonstrated that inhibition of GSK3 as key member of the destruction complex leads to the stabilization of YAP/TAZ in mouse embryonic stem cells (40). Based on this model, we would have expected an increase of YAP/TAZ levels under treatment with LY2090314. On the contrary, we measured a significant decrease of YAP/TAZ levels in pancreatic cancer cells treated with GSK3 inhibitors. Moreover, we measured a significant increase in β-catenin levels in cells silenced for TAK1 expression, indicating an inactivation and not a stabilization of the destruction complex in these models. These results suggest that in pancreatic cancer the role of TAK1 activation in sustaining YAP/TAZ stability is probably more relevant than their recruitment within the destruction complex.

In conclusion, our study demonstrates for the first time a crucial role for TAK1 in controlling the activity of YAP/TAZ in pancreatic cancer. Targeting TAK1 through the inhibition of GSK3 could be a promising approach to modulate the oncogenic functions, ad in particular the chemoresistance, sustained by YAP/TAZ in this disease. Our results candidate LY2090314 as a novel agent that warrants further clinical development in integrated therapeutic strategies (41) with chemotherapeutic agents such as nab-paclitaxel for the treatment of pancreatic cancer.

Disclosure of Potential Conflicts of Interest

No potential conflicts of interest were disclosed.

Authors' Contributions

Conception and design: R. Santoro, M. Zanotto, C. Zecchetto, G. Piro, D. Melisi
Development of methodology: G. Piro, D. Melisi
Acquisition of data (provided animals, acquired and managed patients, provided facilities, etc.): R. Santoro, M. Zanotto, F. Simionato, V. Merz, C. Cavallini, F. Sabbadini, F. Boschi, A. Scarpa, D. Melisi
Analysis and interpretation of data (e.g., statistical analysis, biostatistics, computational analysis): R. Santoro, M. Zanotto, G. Piro, F. Boschi, D. Melisi
Writing, review, and/or revision of the manuscript: R. Santoro, C. Zecchetto, V. Merz, A. Scarpa, D. Melisi
Administrative, technical, or material support (i.e., reporting or organizing data, constructing databases): D. Melisi
Study supervision: C. Zecchetto, D. Melisi

Acknowledgments

This work was supported by the investigator grants nos. 19111 and 23719 and 5×1000 grant no. 12182 through the Associazione Italiana per la Ricerca sul Cancro (AIRC), by the Ricerca Finalizzata 2016 grant through the Italian Ministry of Health, and by the "Nastro Viola" and "Voglio il Massimo" associations of patients' donations to D. Melisi. Part of the work was performed at the Laboratorio Universitario di Ricerca Medica (LURM) Research Center, University of Verona. We thank Drs. Michela Deiana, Maria Teresa Valenti, Carmine Carbone, and Lorena Torroni for technical help and Dr. Hayley Louise Salt for data entry and administrative support. We thank Prof. Jae-Hyuck Shim for the kind gift of murine wild-type and kinase-dead K63W TAK1 lentiviral expression constructs.

The costs of publication of this article were defrayed in part by the payment of page charges. This article must therefore be hereby marked *advertisement* in accordance with 18 U.S.C. Section 1734 solely to indicate this fact.

Received March 22, 2019; revised July 19, 2019; accepted September 18, 2019; published first September 27, 2019.

References

1. Melisi D, Calvetti L, Frizziero M, Tortora G. Pancreatic cancer: systemic combination therapies for a heterogeneous disease. Curr Pharm Des 2014;20:6660–9.
2. Vaccaro V, Sperduti I, Vari S, Bria E, Melisi D, Garufi C, et al. Metastatic pancreatic cancer: is there a light at the end of the tunnel? World J Gastroenterol 2015;21:4788–801.
3. Tamburrino A, Piro G, Carbone C, Tortora G, Melisi D. Mechanisms of resistance to chemotherapeutic and anti-angiogenic drugs as novel targets for pancreatic cancer therapy. Front Pharmacol 2013;4:56.
4. Zhang W, Nandakumar N, Shi Y, Manzano M, Smith A, Graham G, et al. Downstream of mutant KRAS, the transcription regulator YAP is essential for neoplastic progression to pancreatic ductal adenocarcinoma. Sci Signal 2014;7:ra42.
5. Shao DD, Xue W, Krall EB, Bhutkar A, Piccioni F, Wang X, et al. KRAS and YAP1 converge to regulate EMT and tumor survival. Cell 2014;158:171–84.
6. Kapoor A, Yao W, Ying H, Hua S, Liewen A, Wang Q, et al. Yap1 activation enables bypass of oncogenic Kras addiction in pancreatic cancer. Cell 2014;158:185–97.
7. Bae JS, Kim SM, Lee H. The Hippo signaling pathway provides novel anti-cancer drug targets. Oncotarget 2017;8:16084–98.
8. Piccolo S, Dupont S, Cordenonsi M. The biology of YAP/TAZ: hippo signaling and beyond. Physiol Rev 2014;94:1287–312.
9. Santoro R, Carbone C, Piro G, Chiao PJ, Melisi D. TAK-ing aim at chemoresistance: the emerging role of MAP3K7 as a target for cancer therapy. Drug Resist Updat 2017;33–35:36–42.

10. Zhuang Z, Ju HQ, Aguilar M, Gocho T, Li H, Iida T, et al. IL1 receptor antagonist inhibits pancreatic cancer growth by abrogating NF-kappaB activation. Clin Cancer Res 2016;22:1432–44.
11. Carbone C, Melisi D. NF-kappaB as a target for pancreatic cancer therapy. Expert Opin Ther Targets 2012;16:S1–10.
12. Melisi D, Chiao PJ. NF-kappa B as a target for cancer therapy. Expert Opin Ther Targets 2007;11:133–44.
13. Melisi D, Xia Q, Paradiso G, Ling J, Moccia T, Carbone C, et al. Modulation of pancreatic cancer chemoresistance by inhibition of TAK1. J Natl Cancer Inst 2011;103:1190–204.
14. Piro G, Giacopuzzi S, Bencivenga M, Carbone C, Verlato G, Frizziero M, et al. TAK1-regulated expression of BIRC3 predicts resistance to preoperative chemoradiotherapy in oesophageal adenocarcinoma patients. Br J Cancer 2015;113: 878–85.
15. Bang D, Wilson W, Ryan M, Yeh JJ, Baldwin AS. GSK-3alpha promotes oncogenic KRAS function in pancreatic cancer via TAK1-TAB stabilization and regulation of noncanonical NF-kappaB. Cancer Discov 2013;3:690–703.
16. Fechtner S, Fox DA, Ahmed S. Transforming growth factor beta activated kinase 1: a potential therapeutic target for rheumatic diseases. Rheumatology 2017;56: 1060–8.
17. Rabba AK, Si L, Xue K, Li M, Li G. In Situ intestinal perfusion of irinotecan: application to P-gp mediated drug interaction and introduction of an improved HPLC assay. J Pharm Pharm Sci 2011;14:138–47.
18. Melisi D, Ossovskaya V, Zhu C, Rosa R, Ling J, Dougherty PM, et al. Oral poly (ADP-ribose) polymerase-1 inhibitor BSI-401 has antitumor activity and synergizes with oxaliplatin against pancreatic cancer, preventing acute neurotoxicity. Clin Cancer Res 2009;15:6367–77.
19. Carbone C, Piro G, Simionato F, Ligorio F, Cremolini C, Loupakis F, et al. Homeobox B9 mediates resistance to anti-VEGF therapy in colorectal cancer patients. Clin Cancer Res 2017.
20. Shim JH, Greenblatt MB, Xie M, Schneider MD, Zou W, Zhai B, et al. TAK1 is an essential regulator of BMP signalling in cartilage. EMBO J 2009;28: 2028–41.
21. Carbone C, Piro G, Gaianigo N, Ligorio F, Santoro R, Merz V, et al. Adipocytes sustain pancreatic cancer progression through a non-canonical WNT paracrine network inducing ROR2 nuclear shuttling. Int J Obes 2018;42:334–43.
22. Carbone C, Moccia T, Zhu C, Paradiso G, Budillon A, Chiao PJ, et al. Anti-VEGF treatment-resistant pancreatic cancers secrete proinflammatory factors that contribute to malignant progression by inducing an EMT cell phenotype. Clin Cancer Res 2011;17:5822–32.
23. Dalla Pozza E, Dando I, Biondani G, Brandi J, Costanzo C, Zoratti E, et al. Pancreatic ductal adenocarcinoma cell lines display a plastic ability to bidirectionally convert into cancer stem cells. Int J Oncol 2015;46:1099–108.
24. Santoro R, Zanotto M, Carbone C, Piro G, Tortora G, Melisi D. MEKK3 Sustains EMT and stemness in pancreatic cancer by regulating YAP and TAZ Transcriptional Activity. Anticancer Res 2018;38:1937–46.
25. Carbone C, Tamburrino A, Piro G, Boschi F, Cataldo I, Zanotto M, et al. Combined inhibition of IL1, CXCR1/2, and TGFbeta signaling pathways modulates in-vivo resistance to anti-VEGF treatment. Anticancer Drugs 2016;27:29–40.
26. Piro G, Carbone C, Cataldo I, Di Nicolantonio F, Giacopuzzi S, Aprile G, et al. An FGFR3 autocrine loop sustains acquired resistance to trastuzumab in gastric cancer patients. Clin Cancer Res 2016;22:6164–75.
27. Phiel CJ, Klein PS. Molecular targets of lithium action. Annu Rev Pharmacol Toxicol 2001;41:789–813.
28. Lin L, Sabnis AJ, Chan E, Olivas V, Cade L, Pazarentzos E, et al. The Hippo effector YAP promotes resistance to RAF- and MEK-targeted cancer therapies. Nat Genet 2015;47:250–6.
29. Azzolin L, Panciera T, Soligo S, Enzo E, Bicciato S, Dupont S, et al. YAP/TAZ incorporation in the beta-catenin destruction complex orchestrates the Wnt response. Cell 2014;158:157–70.
30. Park HW, Kim YC, Yu B, Moroishi T, Mo JS, Plouffe SW, et al. Alternative Wnt signaling activates YAP/TAZ. Cell 2015;162:780–94.
31. Smit L, Baas A, Kuipers J, Korswagen H, van de Wetering M, Clevers H. Wnt activates the Tak1/Nemo-like kinase pathway. J Biol Chem 2004;279:17232–40.
32. Ishitani T, Ninomiya-Tsuji J, Nagai S, Nishita M, Meneghini M, Barker N, et al. The TAK1-NLK-MAPK-related pathway antagonizes signalling between beta-catenin and transcription factor TCF. Nature 1999;399:798–802.
33. Ishitani T, Kishida S, Hyodo-Miura J, Ueno N, Yasuda J, Waterman M, et al. The TAK1-NLK mitogen-activated protein kinase cascade functions in the Wnt-5a/Ca(2+) pathway to antagonize Wnt/beta-catenin signaling. Mol Cell Biol 2003; 23:131–9.
34. Yu M, Ting DT, Stott SL, Wittner BS, Ozsolak F, Paul S, et al. RNA sequencing of pancreatic circulating tumour cells implicates WNT signalling in metastasis. Nature 2012;487:510–3.
35. Piccolo S, Cordenonsi M, Dupont S. Molecular pathways: YAP and TAZ take center stage in organ growth and tumorigenesis. Clin Cancer Res 2013;19: 4925–30.
36. Sorrentino G, Ruggeri N, Specchia V, Cordenonsi M, Mano M, Dupont S, et al. Metabolic control of YAP and TAZ by the mevalonate pathway. Nat Cell Biol 2014;16:357–66.
37. Mullen PJ, Yu R, Longo J, Archer MC, Penn LZ. The interplay between cell signalling and the mevalonate pathway in cancer. Nat Rev Cancer 2016;16:718–31.
38. Gray JE, Infante JR, Brail LH, Simon GR, Cooksey JF, Jones SF, et al. A first-in-human phase I dose-escalation, pharmacokinetic, and pharmacodynamic evaluation of intravenous LY2090314, a glycogen synthase kinase 3 inhibitor, administered in combination with pemetrexed and carboplatin. Invest New Drugs 2015;33:1187–96.
39. Rizzieri DA, Cooley S, Odenike O, Moonan L, Chow KH, Jackson K, et al. An open-label phase 2 study of glycogen synthase kinase-3 inhibitor LY2090314 in patients with acute leukemia. Leukemia lymphoma 2016;57:1800–6.
40. Azzolin L, Zanconato F, Bresolin S, Forcato M, Basso G, Bicciato S, et al. Role of TAZ as mediator of Wnt signaling. Cell 2012;151:1443–56.
41. Melisi D, Piro G, Tamburrino A, Carbone C, Tortora G. Rationale and clinical use of multitargeting anticancer agents. Curr Opin Pharmacol 2013;13:536–42.